# Investigating the Impact of Substrate Composition on 3D Printed mmWave CSRR Sensor

Jeevan Persad[1], Sean Rocke[1], Aaron Roopnarine[1], Azim Abdool[1]
1. Department of Electrical & Computer Engineering, The University of The West Indies, Trinidad & Tobago
(Email: Jeevan.Persad@sta.uwi.edu)

## Abstract

**Diabetes is a chronic noncommunicable disease which lays a heavy burden on many impoverished communities globally. The ability to monitor and manage the disease is one key component to lessening its impact. 3D printing (3DP) offers an economical manufacturing method to produce medical sensors for these communities. However, sensor design for 3DP is not simple. This work considers a modified millimeter wave (mmWave) sensor based on a complementary split ring resonator (CSRR) topology for non-invasive blood glucose monitoring. The CSRR sensor has a center frequency of 61.2GHz and is designed to be constructed on a Nylon substrate using 3DP. Two established heterogenous mixture models, Landau & Lifshitz, Looyenga and Rayleigh, were chosen to evaluate the relative effective permittivity of the Nylon substrate for varying infill percentages. The mixture models were calculated using MATLAB simulation and produced different values for effective permittivity for a range of infill percentages. The CSRR sensor was investigated using COMSOL Multiphysics in order to evaluate the impact of the effective permittivity variations. Simulation results demonstrate variations in reflection coefficient (S11) of up to 1.5dB and resonant frequency of up to 1.25GHz. Therefore, the mixture model must match the 3DP process to avoid significant deviation between the simulated and actual sensor. These results have significant implications when designing a wide array of sensor structures for 3DP over a variety of operating frequency bands.**

***Keywords—mmWave; complementary spit ring resonators; 3D printing; non-invasive monitoring; glucose estimation***

## Introduction

Electronics manufacturers continue to face pressures stemming from shorter times to market and rapid upgrading of functionality, coupled with sustained consumer demands toward smaller, more powerful and feature rich devices. These pressing demands have motivated the investigation of alternative mechanisms for electronics manufacturing [1]-[2]. Printed electronics offer the possibility to disrupt the traditional photolithographic/subtractive manufacturing line with simpler additive processes. Additive electronics manufacturing, which utilizes 3D printing (3DP) techniques, allows for fewer production steps and significant reduction in material wastage [3]. In particular, the so called Direct Digital (DD) processes such as Inkjet Printing, Aerosol and Multijet Printing allow for the potential manufacture of the Printed Circuit Board (PCB) straight from the digital file in a single processing step [3]-[5]. A common electronics manufacturing application of DD 3DP processes is the creation of the dielectric substrate needed for the electronics assemblies. A number of researchers have employed various DD processes to produce example electronic dielectrics. A good discussion on these works can be found in [6]. The 3DP dielectric substrate can potentially allow for improved benefits including increased flexibility and reduced weight compared to traditional dielectrics used in conventional electronics manufacture (such as FR4).

One common area of application for DD 3DP dielectric substrates is bio-sensors where the ability to produce complex, lightweight and flexible structures can improve fit and comfort of the sensor structure [26]. In the most general sense, a bio-sensor can be considered to be an analytical device which converts a biological phenomenon into an electrical output [7]. For this study, a complementary split ring resonator (CSRR) structure was adopted from previous work by [8] and modified to operate in the millimeter wave (mmWave), 61 – 61.5GHz industrial, scientific and medical (ISM) band. The target end application of this CSRR structure is non-invasive monitoring of tissue glucose levels. Non-invasive methods of glucose monitoring can offer improved comfort for patients over methods which require a blood sample for measurement [9]. MmWave technology has been shown to be one effective means for non-invasive measuring of complex or relative permittivity of biological tissue for glucose monitoring [9]. In the proposed mmWave sensor design, the dielectric substrate material chosen is Nylon which is a common DD 3DP material used in medical applications [10]-[11]. The use of the Nylon substrate allows for the potential implementation of a flexible and light sensor. The variation in substrate weight is achieved through the ability of the DD 3DP process to modify the percentage infill of the constructed dielectric substrate [13]. The Nylon substrate with its modified infill would also experience variation in the electromagnetic (EM) properties such as effective (complex) permittivity, permeability and conductance. The resultant EM properties can be determined through the use of mixture models which facilitate calculation of the equivalent substrate properties based on the known properties of the constituent materials [14]-[16]. However, the predicted EM properties, such as permittivity and permeability, vary based on the chosen mixture model. It is therefore important to characterize the EM behaviour of sensors which are produced via DD 3DP processes. To the best of the authors' knowledge there is limited work in this area.

In this study, values of the resultant permittivity ($\epsilon_{eff}$) for the modified Nylon substrate for varying infill percentages are calculated based on two selected mixture models using the MATLAB® simulation software. The consequent impact on the performance of the CSRR sensor due to the difference in the calculated resultant permittivity values was evaluated using the

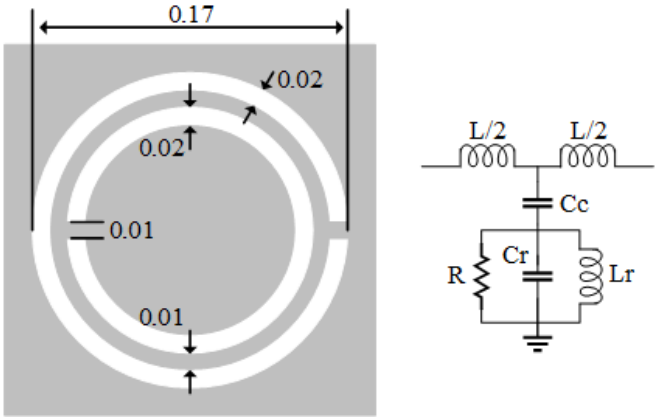


**Figure 1.** Dimensions (mm) and equivalent circuit for the CSRR sensor

COMSOL Multiphysics® software suite. The results and discussion highlight the differences arising based upon which mixture model is used and the consequent variation in the predicted performance of the CSRR sensor. Furthermore, a case is made for investigation of the EM behaviour of 3DP sensors in general.

## Theory & Background

The theory and background will briefly describe the design and dimensions of the CSRR sensor as well as the simulation model which was constructed for the study. The mixture models used for evaluating the varying percentage infill of the Nylon substrate will also be introduced. Finally, this section will also describe the COMSOL Multiphysics® resources used for the study including details of the simulation setup.

### CSRR Sensor Design & Operation

Figure 1 illustrates the dimensions and equivalent circuit for the modified mmWave CSRR sensor [8] designed for operation within the 61 – 61.5GHz band on a Nylon dielectric substrate with 100% infill. The Nylon dielectric substrate is specified as 0.8mm thick. Suitable dimensions of the CSRR sensor for tuning to operate within the ISM band of interest were established using the COMSOL Multiphysics® software suite. The dimensional and electrical details of the sensor model are captured in Table1.

**Table 1.** COMSOL® model details

| Item | Dimensions | Electrical Parameters |
|---|---|---|
| Microstrip | Trace width: 50 Ω impedance matched [24]<br>Trace length: 30.0mm | Perfect electric conductor |
| Substrate (Nylon) | 15.0mm, 30.0mm, 0.8mm | σ = 10e-12 S/m<br>$\boldsymbol{\epsilon}_{eff}$ = set by mixture model calculation |
| Epidermis | 15.0mm, 30.0mm, 1.0mm | σ = 1.8e-2 S/m<br>$\boldsymbol{\epsilon}_r$ = 31 [25] |
| Air | Single layer sphere<br>Layer thickness: 10mm<br>Radius: 60mm | |

The COMSOL RF Module was identified as suitable for the studying owing to the frequencies of interest being in the mmWave range. The resonant frequency of the sensor ($f_r$) may be described by [8]:

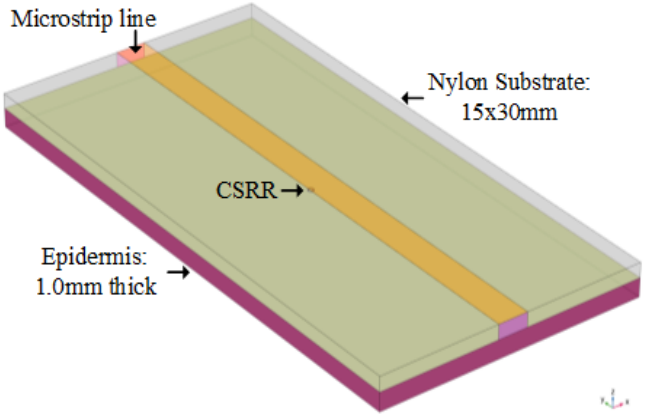


**Figure 2.** COMSOL Multiphysics® model used to optimise the CSRR sensor

$$f_r = \frac{1}{2\pi\sqrt{Lr(Cc+Cr)}} \quad (1)$$

where $Lr$ and $Cr$ are the CSRR inductance and capacitance respectively; $Cc$ is the microstrip line coupling capacitance and $L$ is the line inductance. The CSRR sensor utilizes the perturbation cavity method to measure the change in the resonant frequency ($\Delta f_r$) induced by the variation in the permittivity of the material under test (MUT). For the purpose of non-invasive tissue glucose monitoring, the MUT is the patient tissue and permittivity changes are induced by variations in concentration of glucose in the tissue [23]. Therefore, a critical component of the measurement accuracy of the CSRR sensor is $f_r$ which in turn is dependent on the sensor's geometry and the EM properties of the sensor material. One important EM property is the permittivity of the sensor dielectric substrate.

The COMSOL Multiphysics® model is illustrated in Figure 2 and shows the sensor against an epidermis layer with an in vivo thickness of 1mm. The model assumes that the sensor structure is fully in contact with the epidermis and the EM properties of the epidermis layer remain constant. These assumptions were adopted since the focus of the study is to examine the performance of the sensor due to variations in the EM properties of the sensor's substrate caused by the changes in percentage infill. The CSRR sensor was excited using the microstrip line and a single lumped excitation port which was optimized using the simulation software. The model was solved for different $\epsilon_{eff}$ values as calculated by the mixture model expressions. For each $\epsilon_{eff}$ a frequency sweep of 50 – 65GHz of the excitation frequency of the CSSR sensor was conducted and the resonant frequency ($f_r$) response and S-parameter (S11) were evaluated.

### Mixture Models

Permittivity ($\epsilon$) can be considered to describe how the dielectric properties of a medium affect and are affected by an electric field which acts upon it. This can be expressed as [17]:

$$\epsilon = \epsilon' - j\epsilon'' = \epsilon_0\epsilon_r * (1 - jtan\delta_\epsilon) \quad (2)$$

Existing DD 3DP printers produce the infill pattern with distinct areas of material and air [27]. Therefore, the Nylon substrate can be considered a binary mixture of two heterogenous

materials (Nylon and air). In the case of varying percentage infill, the Nylon would be considered to be the matrix material and the air gaps would be considered to be the inclusions. For the purpose of this study, two heterogenous mixture models were considered [18]: Landau & Lifshitz, Looyenga (LLL) and Rayleigh (RAY). Relative permittivity values for Nylon and air [19] were incorporated into the effective permittivity mixture models for percentage Nylon infills varying between 10 % and 100% infill in steps of 10%.

*1) Landau & Lifshitz, Looyenga (LLL):* The expression for complex permittivity derived independently by Looyenga and Landau and Lifshitz [20]-[21] implies a cubed root relationship existing between the constituent and mixture permittivities:

$$(\epsilon_{eff})^{1/3} = v_1(\epsilon_1)^{1/3} + v_2(\epsilon_2)^{1/3} \quad (3)$$

where $v_1$, $\epsilon_1$ are the volume and relative permittivity of the first material (Nylon) and $v_2$, $\epsilon_2$ are the volume and relative permittivity of the second material (air).

*2) Rayleigh (RAY):* This mixture model is expressed as [22]:

$$\frac{\epsilon_{eff}-\epsilon_1}{\epsilon_{eff}+2\epsilon_1} = v_2 \frac{\epsilon_2-\epsilon_1}{2\epsilon_1+\epsilon_2}, \quad (4)$$

where $\epsilon_1$is the relative permittivity of the mixture matrix and $v_2$, $\epsilon_2$ are the volume and relative permittivity of the inclusion material. The respective expressions for the mixture models were encoded using the MATLAB® simulation software to calculate the values of $\epsilon_{eff}$. The LiveLink™ module in COMSOL® allowed for the importation of the MATLAB® data into the CSRR sensor model for the frequency domain study using the COMSOL® RF module.

## Results & Discussion

Figure 3 shows the calculated values for $\epsilon_{eff}$ based on the percentage infill of the Nylon dielectric substrate of the CSRR sensor for the LLL and RAY mixture models. For all infill percentages (except 100% infill) the RAY model generated higher values for $\epsilon_{eff}$ with the greatest deviation of 0.08 observed for the 50% infilled dielectric substrate.

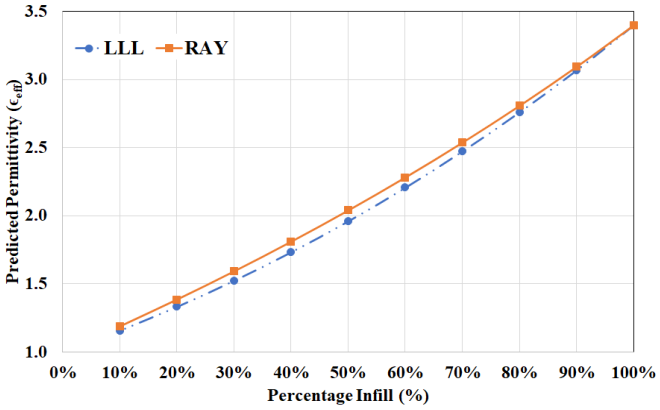


**Figure 3.** Predicted $\epsilon_{eff}$ for the various percentage infill for LLL and RAY mixture models

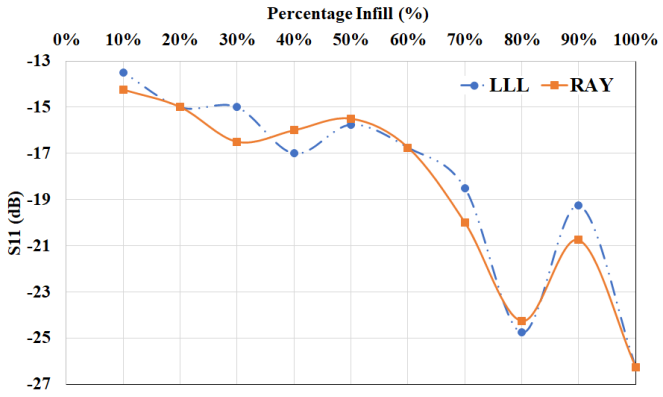


**Figure 4.** Simulated S11 for the various percentage infill for LLL and RAY mixture models

Figure 4 shows the simulated values of S11 at resonance versus the different percentage infill of the Nylon substrate for the two mixture models. Both mixture models showed an overall trend of S11 decreasing in value from a maximum value at 10% infill (which corresponds to a minimum value of $\epsilon_{eff}$). In addition, while the overall trend showed a decrease in S11, the variation was nonlinear. This result implies that any attempt to reduce the infill of the sensor substrate will result in deterioration in performance due to increased mmWave reflection. Also, of interest was the fact that the incremental difference in the predicted values of $\epsilon_{eff}$ for the RAY and LLL mixture models for select values of percentage infill produced significant varaitions in S11. The greatest differences in the S11 values for the two mixture model predictions was 1.5dB and this was observed at 30, 70, 90% infill. These results are significant since they underline the difficulty in predicting the resultant S11 value of the sensor for an incremental difference in the predicted $\epsilon_{eff}$ due to the two different mixture models.

Figure 5 shows the simulated values of $f_r$ versus the different percentage infill of the substrate for the two mixture models. The $f_r$ values were seen to decrease as the percentage infill was reduced. The observed trend in the values of $f_r$ was nonlinear. The values of $f_r$ for the RAY and LLL mixture models diverged as expected from the point of 100% infill. The greatest variations of 1.20GHz and 1.25GHz were observed at 40% and 50% infill respectively, which corresponds to the maximum deviation of $\epsilon_{eff}$ in the mixture models at the 50% infill mark. The CSRR sensor's ability to measure and quantify the

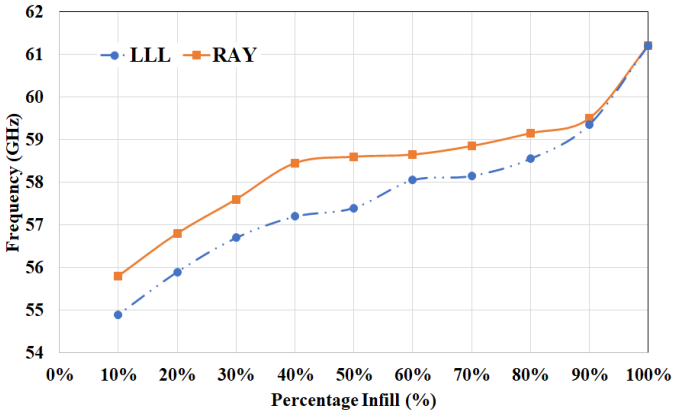


**Figure 5.** Simulated resonant frequency for the various percentage infill for LLL and RAY mixture models

permittivity of the patient tissue and by extension the glucose concentration is dependent on the measured value for $\Delta f_r$. The significant variation in the values of $f_r$ as a result of the difference in the $\epsilon_{eff}$ predicted by the two mixture models for each percentage infill would limit the ability to accurate design the CSRR sensor. The resultant variations in design will contribute to significant differences in performance of the final manufactured CSRR sensor.

## Conclusion

The CSRR mmWave sensor was designed with a Nylon dielectric substrate with 100% infill for operation at 61.2GHz. The sensor was subsequently modeled with varying percentage infill applied to the Nylon substrate. For small differences in the $\epsilon_{eff}$ of the Nylon substrate, as predicted by the LLL and RAY mixture models, significant variations were observed in the S11 response and $f_r$. Therefore, an appropriate mixture model for use in modeling and design of a DD 3DP substrate must be established since any variation in the model predictions and the actual substrate will result in significant variations between the designed and actual sensor. The resultant variation in the sensor characteristics (such as the resonant frequency) due to the variation in the percentage infill, highlight the potential to tune the substrate material and by extension the sensor response. As ongoing work, additional evaluation of suitable mixture models will be undertaken in conjunction with the testing of a statistically significant number of DD 3DP samples. This future work will allow for the effective use of mixture models when designing sensor structures which are intended to be produced using DD 3DP technologies. The ability to tune the substrate through variation of infill percentage will also be investigated with an emphasis on achieving highly localised and controlled variations in the EM characteristics of the material and by extension the response of the sensor structure.

## References


1. A. Espera, J. Dizon, Q. Chen and R. Advincula, "3D-printing and advanced manufacturing for electronics", *Progress in Additive Manufacturing*, **vol. 4**, no. 3, pp. 245-267, (2019)
2. N Gupta, C Weber, S Newsome, "Additive manufacturing: status and opportunities." *Science and Technology Policy Institute*, Washington, (2012)
3. E. Macdonald et al., "3D Printing for the Rapid Prototyping of Structural Electronics," *IEEE Access*, **vol. 2**, pp. 234-242, Dec. (2014)
4. G. Cummins and M. Desmulliez, "Inkjet printing of conductive materials: a review", *Circuit World*, **vol. 38**, no. 4, pp. 193-213, (2012)
5. A. A. Gupta, A. Bolduc, S. G. Cloutier and R. Izquierdo, "Aerosol Jet Printing for printed electronics rapid prototyping," 2016 *IEEE International Symposium on Circuits and Systems (ISCAS)*, Montreal, QC, pp. 866-869, (2016)
6. U. Caglar, "Studies of inkjet printing technology with focus on electronic materials," Tampereen teknillinen yliopisto. Julkaisu-Tampere University of Technology. Publication; 863, (2010)
7. P. Coulet and L. Blum, *Biosensor Principles and Applications*, New York: CRC Press, (2019)
8. M. A. H. Ansari, A. K. Jha and M. J. Akhtar, "Design and Application of the CSRR-Based Planar Sensor for Noninvasive Measurement of Complex Permittivity," *IEEE Sensors Journal*, **vol. 15,** no. 12, pp. 7181-7189, Dec. (2015)
9. W. Villena Gonzales, A. Mobashsher and A. Abbosh, "The Progress of Glucose Monitoring—A Review of Invasive to Minimally and Non-Invasive Techniques, Devices and Sensors", *Sensors*, **vol. 19,** no. 4, p. 800, (2019)
10. F. Zhang, S. Cho, S. Yang, S. Seo, G. Cha and H. Nam, "Gold Nanoparticle-Based Mediatorless Biosensor Prepared on Microporous Electrode", *Electroanalysis*, **vol. 18,** no. 3, pp. 217-222, (2006)
11. V. Ferrara et al., "DNA-Based Biosensor on Flexible Nylon Substrate by Dip-Pen Lithography for Topoisomerase Detection", *Lecture Notes in Electrical Engineering*, pp. 309-316, (2019)
12. J. Yoon, H. Cho, M. Shin, H. Choi, T. Lee and J. Choi, "Flexible electrochemical biosensors for healthcare monitoring", *Journal of Materials Chemistry B*, (2020)
13. L. Baich, G. Manogharan and H. Marie, "Study of infill print design on production cost-time of 3D printed ABS parts", *International Journal of Rapid Manufacturing*, **vol. 5,** no. 34, p. 308, (2015)
14. R. Cret, L. Darabant, C. Farcas, and A. Turcu, "Considerations about the influence of some factors related to the geometric characteristics of inclusions on effective permittivity of dielectric mixtures," *Advanced Topics in Electrical Engineering (ATEE)*, 2011 7th International Symposium on. IEEE, pp. 1–6, (2011)
15. E. Tuncer and S. M. Gubanski, "Dielectric properties of different composite structures," in International Conference on Dielectric and Related Phenomena'98. *International Society for Optics and Photonics*, pp. 136–142, (1999)
16. B. Sareni, L. Kr¨ahenb¨uhl, A. Beroual, and C. Brosseau, "Effective dielectric constant of random composite materials," *Journal of Applied Physics*, **vol. 81**, no. 5, pp. 2375–2383, (1997)
17. B. Notaros, Conceptual electromagnetics. Boca Raton: CRC Press, (2017)
18. S. O. Nelson, "Estimating the permittivity of solids from measurements on granular or pulverized materials," *MRS Proceedings*, **vol. 124**. Cambridge Univ Press, p. 149, (1988)
19. S. Chen, J. Kupershmidt, K. A. Korolev and M. N. Afsar, "A High-Resolution Quasi Optical Spectrometer for Complex Permittivity and Loss Tangent Measurements at Millimeter Wavelengths," *IEEE Instrumentation & Measurement Technology Conference IMTC 2007*, Warsaw, pp. 1-5, (2007)
20. H. Looyenga, "Dielectric constants of heterogeneous mixtures," *Physica*, **vol. 31**, no. 3, pp. 401–406, (1965)
21. L. Landau, E. Lifšic and L. Pitaevskij, Electrodynamics of continuous media. Amsterdam: *Elsevier Butterworth-Heinemann*, (2009)
22. L. Rayleigh, "Lvi. on the influence of obstacles arranged in rectangular order upon the properties of a medium," *The London, Edinburgh, and Dublin Philosophical Magazine*

*and Journal of Science*, **vol. 34**, no. 211, pp. 481–502, (1892)
23. J. Yeo and J. Lee, "High-Sensitivity Microwave Sensor Based on An Interdigital-Capacitor-Shaped Defected Ground Structure for Permittivity Characterization", *Sensors*, **vol. 19**, no. 3, p. 498, (2019)
24. RF, e., Calculators, R. and Calculator, M., 2020. Microstrip Impedance Calculator. [online] Everythingrf.com. Available at: <https://www.everythingrf.com/rf-calculators/microstrip-impedance-calculator> [Accessed 31 August 2020].
25. Niremf.ifac.cnr.it. 2020. Dielectric Properties Of Body Tissues: Home Page. [online] Available at: <http://niremf.ifac.cnr.it/tissprop/> [Accessed 31 August 2020].
26. T. Han, S. Kundu, A. Nag and Y. Xu, "3D Printed Sensors for Biomedical Applications: A Review", *Sensors*, **vol. 19**, no. 7, p. 1706, (2019)
27. A. Goulas et al., "The Impact of 3D Printing Process Parameters on the Dielectric Properties of High Permittivity Composites", *Designs*, **vol. 3**, no. 4, p. 50, (2019)